



Empirical models of daily and monthly global solar irradiation using sunshine duration for Alagoas State, Northeastern Brazil



José Leonaldo De Souza^{a,*}, Gustavo Bastos Lyra^b, Cícero Manoel Dos Santos^a,
Ricardo Araujo Ferreira Junior^c, Chigueru Tiba^d, Guilherme Bastos Lyra^c,
Marco Antonio Maringolo Lemes^a

^a Laboratório de Agrometeorologia e Radiometria Solar, Instituto de Ciências Atmosféricas, Universidade Federal de Alagoas, Campus A.C. Simões, BR 104-Norte, Km 97, Tabuleiro dos Martins, CEP 57072-970 Maceió, Alagoas, Brazil

^b Departamento de Ciências Ambientais, Instituto de Florestas, Universidade Federal Rural do Rio de Janeiro, Rod. BR 465, Km 7, CEP 23890-970, Seropédica, Rio de Janeiro, Brazil

^c Laboratório de Agrometeorologia e Radiometria Solar, Centro de Ciências Agrárias, Universidade Federal de Alagoas, Campus A.C. Simões, BR 104-Norte, Km 97, Tabuleiro dos Martins, CEP 57072-970 Maceió, Alagoas, Brazil

^d Departamento de Energia Nuclear, Universidade Federal de Pernambuco, Av. Prof. Luiz Freire, 1000-CDU, CEP 50.740-540 Recife, Pernambuco, Brazil

ARTICLE INFO

Article history:

Received 13 March 2015

Revised 27 November 2015

Accepted 7 January 2016

Keywords:

Ångström–Prescott
Sunshine duration
Solar irradiation
Northeastern Brazil
Empirical models

ABSTRACT

The Ångström–Prescott model called M1 together with ten modified versions, all based on the sunshine duration were adjusted to estimate the daily global and monthly averaged solar irradiation for some sites in the hinterland of Alagoas State in the eastern coast of the Northeastern Brazil. The models were adjusted with meteorological data from 2007 to 2010 and their skills were analyzed using: the Mean Bias Error, Root Mean Square Error and Willmott's Index of Agreement. The results indicate that the fitted coefficients depend on the geographical coordinates, altitude and local microclimate with 15% differences among the coefficients and estimates. The largest errors are observed in the regions with more cloudiness. Mean Bias Error and Root Mean Square Error for the daily evaluation of models M1, M9 and M11 were similar, with high values of Willmott's Index. The daily estimates obtained with models M1 and M11 did not differ more than 5%. Models M9 and M11 showed a better performance than that of M1 on a monthly basis. Finally, models M1 and M11 yielded the best results and due to their efficiency and simplicity are recommended to estimate the daily and monthly solar irradiation where sunshine duration data are available.

© 2016 Elsevier Ltd. All rights reserved.

Introduction

Surface global solar irradiation (H_g) is used in meteorology, climatology, radiation and energy budgets, water treatment processes, heating and natural lighting, agriculture and forestry and use of renewable energy [1]. Indeed, solar energy seems to be the most important, promising and sustainable form of energy able to mitigate the environmental problems humankind is to face in the future [2]. Despite its unquestionable importance, H_g measurements are not globally operational due to the high cost of acquisition, maintenance, calibration and technical complexities [3,4]. Particularly in Brazil, there are relatively few studies concerning

H_g [6–8] and long time series of this variable are relatively rare, due to the continental size of the country [9].

The most appropriated method to quantify H_g is to use pyrometer data [10]. However, empirical methods that employ meteorological variables (such as air temperature [11,12], water vapor pressure [13], relative humidity [5] and precipitation [14], all cheaply measured) are frequently used to overcome these observational difficulties. The Ångström–Prescott (A–P) [15,16], among many others using sunshine duration as input data, outstands for its simplicity and better statistical performance under different climatic conditions and time scales [17–19]. Some studies suggested that modified models (such as quadratic, cubic, logarithmic and exponential) may improve H_g estimates [20–27].

Empirical models are used to provide solarimetric data series and are useful tools to estimate H_g where measurements are scarce or non-existing [28]. Not all models are capable of estimating H_g correctly under conditions different from those used originally in their development [17,29]. Thus, it is necessary to fit their

* Corresponding author at: Federal University of Alagoas (UFAL), Laboratory of Agrometeorology and Solar Radiometry, Institute of Atmospheric Sciences (LARAS/ICAT), Campus A.C. Simões, BR 104-Norte, Km 97, Tabuleiro dos Martins, Maceió/AL – 57072-970, Brazil. Tel.: +55 82 32141360; fax: +55 82 32141367.

E-mail address: jls@ccen.ufal.br (J.L. De Souza).

coefficients using local data and test them to determine the uncertainties in estimating H_g . Several sites in Brazil have long time series of sunshine duration and these data could be used to estimate H_g with empirical models [30–32]. However, the quality of these estimates depends, again, on a fitting with local data. Tiba [6] estimated Ångström–Prescott model coefficients β_1 and β_2 for sites in Northeastern Brazil (NEB) and noticed a high variability ($0.22 < \beta_1 < 0.35$ and $0.31 < \beta_2 < 0.58$). Andrade-Junior et al. [33] calculated them for the climatic conditions prevailing in Piauí state also in NEB ($\beta_1 = 0.3107$, $\beta_2 = 0.5383$ for the rainy season and $\beta_1 = 0.3130$, $\beta_2 = 0.5086$ for the dry season). They did not notice any statistically significant difference when seasonal or annual coefficients were used.

Jerszurki and Souza [34] observed similar results for other regions of Brazil [($0.17 < \beta_1 < 0.23$ and $0.35 < \beta_2 < 0.45$) for the monthly scale and ($\beta_1 = 0.19$ and $\beta_2 = 0.41$) for the annual scale in Paraná state, southern Brazil]. Daniele et al. [35] obtained $0.241 < \beta_1 < 0.345$ and $0.430 < \beta_2 < 0.515$ (monthly scale) and $\beta_1 = 0.278$, $\beta_2 = 0.498$ (annual scale) for Brasília DF in central Brazil. Carvalho et al. [36] obtained $0.252 < \beta_1 < 0.299$ and $0.397 < \beta_2 < 0.504$ (monthly scale) and $\beta_1 = 0.295$, $\beta_2 = 0.417$ (annual scale) for Seropédica in Rio de Janeiro, southeastern Brazil. There were no statistically significant differences regarding the use of monthly and annual coefficients in these studies. Despite its location in NEB, studies on the adjustment of empirical models (such as those considered here) are scarce for Alagoas region. Furthermore, long time series of H_g as estimated from the sunshine duration are used to quantify its time and space variability what is essential in designing solar energy plants and agricultural projects.

In the present study, the Ångström–Prescott model and seven modified versions [20–26] are adjusted and assessed on both daily and monthly scales for three sites: Água Branca, Pão de Açúcar and Palmeira dos Índios in the interior of Alagoas State. In addition, three other models are proposed. The model coefficients are fitted with local data to yield the best estimate for each of these sites and sensitivity studies to prevailing weather systems and climate patterns were carried out.

Materials and methods

Sites and data

The daily measurements of H_g and sunshine duration (n) at Água Branca, Pão de Açúcar and Palmeira dos Índios were obtained at the solarimetric stations (Fig. 1), for the 2007–2010 period. The Brazilian Instituto Nacional de Meteorologia (INMET) using conventional Campbell–Stokes heliographs provided sunshine duration series (in hours).

Daily global solar irradiation (H_g^d , in MJ m^{-2}) were obtained by integrating (trapezoidally method) the daily solar irradiance (I_g , in W m^{-2}) between 06:00 LT and 17:00 LT (Local Time) Eq. (1). I_g was measured using black and white Eppley pyranometer [dependence on temperature: $\pm 1.5\%$ (-20°C to $+40^\circ\text{C}$); linearity: $\pm 1.0\%$, (0 – 1400 W m^{-2}); cosine response: $\pm 2.0\%$ ($0 < \theta_z < 70^\circ$) and $\pm 5.0\%$ ($70 < \theta_z < 80^\circ$); measurement bandwidth: (285 – 2800 nm)]. The pyranometers were connected to a datalogger (CR1000, Campbell Scientific Inc., Logan, Utah) programmed to make measurements every second and store 1 min averaged values [9]:

$$H_g^d = \int_{t_o}^{t_f} I_g^h dt \quad (1)$$

where (I_g^h) is the hourly solar global irradiance and $t_o = 06:00 \text{ LT}$ and $t_f = 17:00 \text{ LT}$. Sunrise and sunset intervals were neglected because of its small contribution to the entire integral.

Monthly averaged global solar irradiation (H_g^m) was calculated using the averaged values of H_g^d for all days in the month:

$$H_g^m = \frac{1}{N'} \sum_{i=1}^{N'} H_g^d \quad (2)$$

where N' is the number of days in the month.

The data were sorted out into two groups; data measured in 2007, 2009 and 2010 were used to fit the model coefficients, and the data collected in 2008 to validate and assess them. This choice was made randomly in order to avoid any trends in the results. Fig. 2 shows the monthly climatological air temperature and rainfall for the three sites, as calculated using data from 1961 to 2010 from INMET.

The climate of Água Branca (in the interior with a mountain like microclimate) according to the Köppen–Geiger classification is “As” – tropical humid, with rainy season during autumn/winter (May to August) and dry season in summer (December to February). The annual air temperature is 23.6°C (20.9°C in July and 25.6°C in December) and annual rainfall is $1,090 \text{ mm}$, with minimum in October (23.9 mm) and maximum in June (193.5 mm) (Fig. 2A). In Palmeira dos Índios, the monthly air temperature changes from 22.6°C (July) to 27.2°C (December) (Fig. 2B), with an annual average of 25.1°C . The total annual precipitation is 881 mm with a minimum in November (13.9 mm) and maximum in June (173 mm). The climate is also classified as “As” – Tropical Humid. The climate of Pão de Açúcar is “Bsh” – Dry Climate (annual rainfall of 591 mm ranging from 13.4 mm in November to 94.2 mm in June) (Fig. 2C) with the dry season in summer and monthly air temperature of 24.9°C (August) and 29.8°C (December) and annual average of 27.5°C .

Ångström–Prescott model and its modified versions

In 1924 Ångström [15] suggested a simple linear relation between the expected H_g^d in a cloudless day and daily maximum sunshine or daylight hours (N) and in 1940, Prescott [16] included the extraterrestrial solar irradiation (H_o) using Eq. (3) (Model M1):

$$\frac{H_g}{H_o} = \beta_1 + \beta_2 \left(\frac{n}{N}\right) \quad (3)$$

The empirical coefficients (β_1 and β_2) are normally fitted using linear regression ($Y = \beta_1 + \beta_2 X$), so $Y = H_g/H_o$ and $X = n/N$. The first coefficient may be interpreted physically as the fraction of the H_g reaching the Earth’s surface in an overcast day and depends mainly on the type and thickness of the clouds [37]. It is a difficult task to estimate it accurately, due to the ceaseless atmospheric motions [38]. The other coefficient (β_2) is a complement that gives the total of H_g . Their sum, ($\beta_1 + \beta_2$), is the potential fraction of solar irradiation at the top of the atmosphere available to reach the surface (that is, H_g in a clear day). Therefore, this sum is affected by the optical thickness, composition and interaction of the air constituents. During its penetration in the atmosphere, the solar radiation is scattered by air molecules, water (in its three phases) and aerosols or particulates. The extent of the dispersion depends on the number and size [with respect to the wave length, (λ)] [39].

Modifications introduced in the original Ångström–Prescott model in order to make it usable in different sites and under climatic conditions yielded other models. Table 1 shows eleven models all based on sunshine which were assessed in this work, regarding the estimative of H_g in the daily (H_g^d) and monthly (H_g^m) partitions: quadratic (M2) [20], cubic (M3) [21], logarithmic (M4) [22], linear logarithmic (M5) [23], exponential (M6) [24], linear exponential (M7) [25] and power (M8) [26]. The senoidal models: (M9) [40], (M10) [41] and (M11) [42] were originally proposed

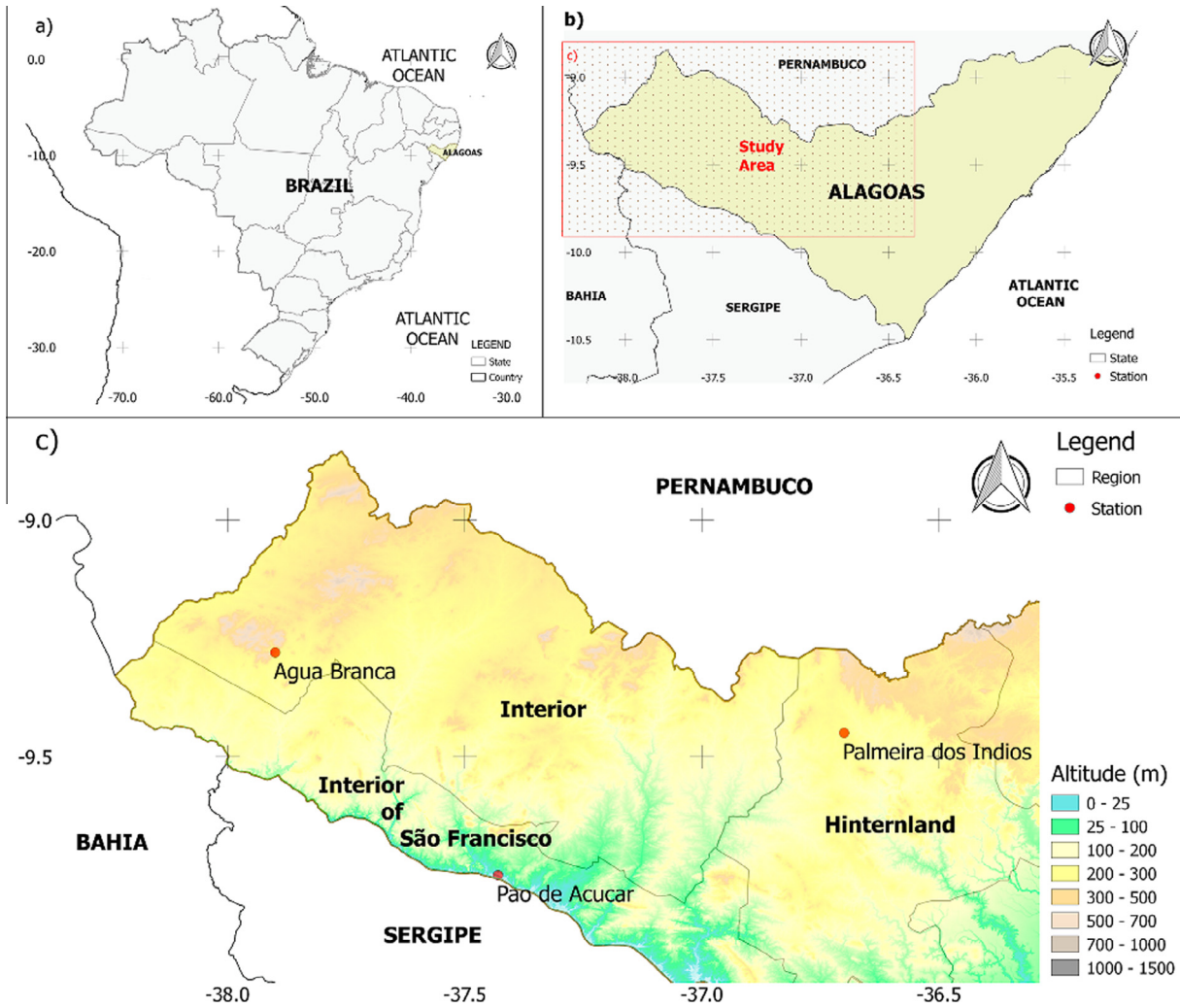


Fig. 1. Meteorological and radiometric stations (c) in the physiographical regions of Alagoas State (b) Northeastern Brazil (a).

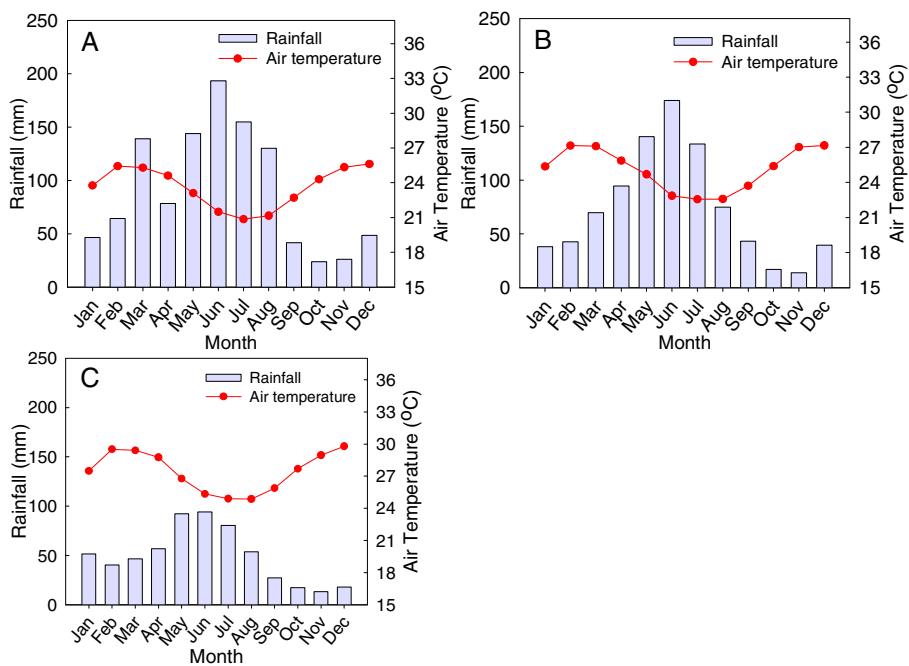


Fig. 2. Climatological distributions (1961–2010) of air temperature and rainfall for (A) Água Branca, (B) Pão de Açúcar and (C) Palmeira dos Índios.

Table 1
Models used in this study.

Model	Type	Equation	Coefficients
M1	Linear	$\frac{H_g}{H_0} = \beta_1 + \beta_2 \left(\frac{n}{N}\right)$	β_1 and β_2
M2	Quadratic	$\frac{H_g}{H_0} = \beta_1 + \beta_2 \left(\frac{n}{N}\right) + \beta_3 \left(\frac{n}{N}\right)^2$	β_1, β_2 and β_3
M3	Cubic	$\frac{H_g}{H_0} = \beta_1 + \beta_2 \left(\frac{n}{N}\right) + \beta_3 \left(\frac{n}{N}\right)^2 + \beta_4 \left(\frac{n}{N}\right)^3$	$\beta_1, \beta_2, \beta_3$ and β_4
M4	Logarithmic	$\frac{H_g}{H_0} = \beta_1 + \beta_2 \log\left(\frac{n}{N}\right)$	β_1 and β_2
M5	Linear-logarithmic	$\frac{H_g}{H_0} = \beta_1 + \beta_2 \left(\frac{n}{N}\right) + \beta_3 \log\left(\frac{n}{N}\right)$	β_1, β_2 and β_3
M6	Exponential	$\frac{H_g}{H_0} = \beta_1 + \beta_2 \exp\left(\frac{n}{N}\right)$	β_1 and β_2
M7	Linear-exponential	$\frac{H_g}{H_0} = \beta_1 + \beta_2 \left(\frac{n}{N}\right) + \beta_3 \exp\left(\frac{n}{N}\right)$	β_1, β_2 and β_3
M8	Power	$\frac{H_g}{H_0} = \beta_1 + \beta_2 \left(\frac{n}{N}\right)^{\beta_3}$	β_1, β_2 and β_3
M9	Senoidal	$\frac{H_g}{H_0} = \beta_1 + \beta_2 \left \sin \left[\frac{\pi}{365} \left(\frac{n}{N} + 5 \right) \right] \right ^{1.5}$	β_1 and β_2
M10	Senoidal	$\frac{H_g}{H_0} = \beta_1 + \beta_2 \sin \left[\frac{2\pi}{\beta_3} \left(\frac{n}{N} \right) + \beta_4 \right]$	$\beta_1, \beta_2, \beta_3$ and β_4
M11	Cossenoidal	$\frac{H_g}{H_0} = \beta_1 + \beta_2 \cos \left[\frac{2\pi}{364} \left(\frac{n}{N} \right) + \beta_3 \right]$	β_1, β_2 and β_3

H_g is the global solar irradiation (MJ m^{-2}), H_0 the global solar irradiation at the top of the atmosphere (MJ m^{-2}), n is the sunshine (h), N is the daylight hours. The coefficients are to be adjusted using local data.

to estimate H_g using Julian calendar with Julian days being replaced by the relative sunshine (n/N). These modifications stemmed from the need to obtain an empirical relation capable of estimating H_g with least deviations and better precision and accuracy. As the solar radiation obeys a periodic pattern in a clear sky day, senoidal (both sines and cossines) functions were deemed to best represent it.

The solar irradiation incident on the top of the atmosphere (H_0) was determined using the equations given in [43], namely:

$$H_0 = \frac{24 \times 3600 \times I_0}{\pi} \left[1 + 0.033 \cos \left(\frac{360 \text{DJ}}{365} \right) \right] \times \left[\left(\frac{\pi}{180^\circ} \omega_s \sin \varphi \sin \delta \right) + (\cos \varphi \cos \delta \sin \omega_s) \right] \quad (4)$$

where I_0 is the solar constant (1367 W m^{-2}), DJ is the Julian day starting on January 1, φ is the local latitude (in degrees), δ is the solar declination (in degrees), given by:

$$\delta = 23.45 \sin \left[\frac{360(\text{DJ} + 284)}{365} \right] \quad (5)$$

and ω_s is the hourly angle (in degrees) given by:

$$\omega_s = \cos^{-1} [-\tan(\delta) \times \tan(\varphi)] \quad (6)$$

The photoperiod or daylight hours (N) is:

$$N = \frac{2}{15} \omega_s \quad (7)$$

The model coefficients were determined by the least square method using MATLAB[®] and were used to estimate H_g and validate the models. This method minimizes the mean square error of the estimates with respect to the observations. The global atmospheric transmittance (k_t) was calculated in order to assess the frequency distribution of local cloudiness. The cloudiness ratio (Φ) gives the number of hours the sun was blocked by clouds [44]. They are, respectively, given by,

$$k_t = \frac{H_g}{H_0} \quad (8)$$

$$\Phi = 1 - \frac{n}{N} = 1 - X \quad (9)$$

where X is the sunshine ratio.

The characterization of sky conditions was adapted from Iqbal [45] and uses local data of cloudiness; it was observed a low

frequency of clear sky ($k_t \geq 0.70$) and cloudy sky ($k_t \leq 0.30$) [43]. The seasonal variation of k_t was classified: cloudy sky ($k_t \leq 0.35$), partially cloudy sky ($0.35 < k_t \leq 0.65$) and clear sky ($k_t > 0.65$).

Statistical parameters

The performance of the models was assessed using statistical indices for measuring the errors: MBE (Mean Bias Error), RMSE (Root Mean Square Error), Willmott index of agreement (d) [46–47], t -test and coefficient of variation (cv). In this order, these parameters are mathematically given by:

$$\text{MBE} = \frac{\sum_{i=1}^{N'} (P_i - O_i)}{N'} \quad (10)$$

$$\text{RMSE} = \left[\frac{\sum_{i=1}^{N'} (P_i - O_i)^2}{N'} \right]^{\frac{1}{2}} \quad (11)$$

$$d = 1 - \frac{\sum_{i=1}^{N'} (P_i - O_i)^2}{\sum_{i=1}^{N'} (|P_i| + |O_i|)^2} \quad (12)$$

where P_i = estimated values of H_g , O_i = measured values of H_g , N' = number of observations, $|P_i|$ = absolute value of the deviation $P_i - \bar{O}_i$, $|O_i|$ = absolute value of the deviation $O_i - \bar{O}_i$, with \bar{O}_i being the average of O_i . The coefficient of variation (cv) is a measure of the data dispersion and is defined as the ratio between the standard deviation (σ) and the average (μ): $\text{cv} = [(\sigma/\mu) * 100]$.

Results and discussions

Global atmospheric transmittance

The monthly averaged k_t , relative sunshine duration and cloudiness ratio are shown in Fig. 3. The monthly and seasonal changes in k_t , n/N and Φ are associated with sky conditions; large (small) values of k_t are related to large (small) values of n/N , as expected from the outputs of Ångström–Prescott model and its modified versions. It was also noticed a relation between the dry (September–March) and rainy (April–August) seasons with respect to the extent of cloudiness and transmittance. The latter was characterized by a larger number of cloudy days and small transmittance values while the opposite occurred for the dry period. The classification of cloudiness using n/N as defined by WMO [48], is: cloudy ($0 \leq n/N < 0.30$), partially cloudy ($0.30 \leq n/N < 0.70$) and clear sky ($0.70 \leq n/N < 1.0$). The averaged sky conditions for the hinterland (Palmeira dos Índios) and interior (Água Branca and Pão de Açúcar) regions of Alagoas State were clear sky (50.65%) followed by partially cloudy sky (38.85%) and cloudy sky (10.50%). This pattern results from the spatial (local topography) and seasonal variability [49].

Changes in k_t give information on the energy availability at the Earth's surface, changes in the local atmospheric conditions [50], besides the frequency distribution and occurrence of cloudier days. This variability is well explained by the local atmospheric conditions with more cloudy days in Winter (rainy season), presence of particulate matter (resulting from slash burnings and natural forest fires, especially in the Summer) and the relative location of large bodies of water (for example, Pão de Açúcar is located along São Francisco River). Occasionally, during the dry season there are some thunderstorms, associated with Upper Air Cyclonic Vortices (UACV) over the coastline of Northeast Brazil [49]. UACV's are persistent weather systems responsible for long periods of rainfall and high cloudiness. The smallest values of k_t (0.531, 0.596 and 0.565, respectively, for Água Branca, Pão de Açúcar and Palmeira dos Índios) observed in February are, probably, associated to UACV's.

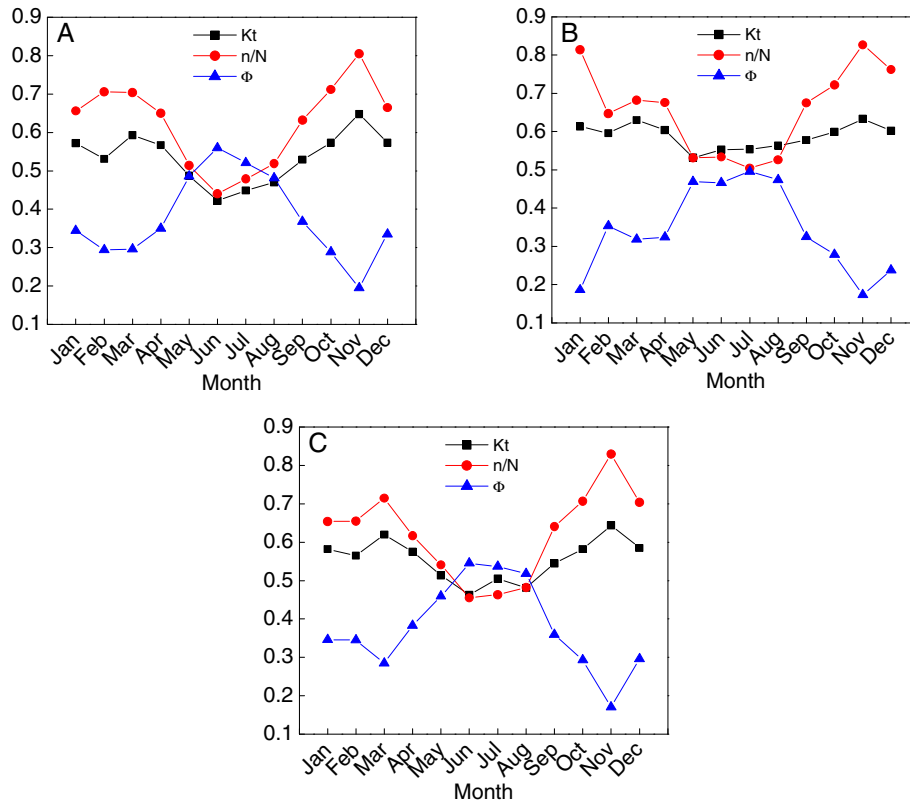


Fig. 3. Monthly averaged changes in the global atmospheric transmittance (k_t), relative sunshine duration ($r = n/N$) and cloudiness ratio (ϕ) at (A) Água Branca, (B) Pão de Açúcar and (C) Palmeira dos Índios.

Monthly means of partially cloudy sky prevailed for the three sites used in this study. November and June were the months with less and more cloudiness, respectively, for Água Branca e Palmeira dos Índios. The highest values of cloudiness were noticed for Pão de Açúcar in May. During partially cloudy sky conditions, the diffuse solar irradiation (H_d) increases with increasing values of H_g . H_g and H_d coincide in an overcast day while the direct solar irradiation (H_d) will be predominant in a day of clear sky. The cloudiness ratio was larger (smaller) during the rainy (dry) periods. This index detected the periods with more (less) cloud coverage in accordance with the k_t analyses. Água Branca and Palmeira dos Índios showed the largest values of ϕ for the rainy season, as expected because the annual rainfall in these two stations is larger than that of Pão de Açúcar [49]. The values of k_t are inversely proportional to ϕ . The decrease in k_t and increase in ϕ are associated with cloudiness changes inherent to seasonal variations. The dry season for these three sites (in Southern Hemisphere) is characterized by lower values of cloudiness and relative humidity and large values of H_g , because the solar rays impinge on the Earth's surface with smaller inclination.

Fitted coefficients on a daily basis

The coefficients of the 11 models used for all sites (Table 2), fitted with daily data are significant up to 5%. They change from place to place with the largest differences being observed for β_1 , β_2 and β_3 of models M5, M7, M9, M10 and M11. The values of the M1 (original Ångström–Prescott model) coefficients for the localities in Alagoas were quite similar to those obtained by Tymvios et al. [51] in Athalassa, semirural region in Cyprus Island ($\beta_1 = 0.199$ and $\beta_2 = 0.538$). However, they differed from those of Liu et al. [38] for 31 sites along the Yellow River in China [$0.11 < \beta_1 < 0.29$] and [$0.50 < \beta_2 < 0.69$] and those of Podestá

et al. [52] for the Pampas in central western part of Argentina (average values of $\beta_1 = 0.214$ and $\beta_2 = 0.571$). Tiba [6] calculated these coefficients for 34 localities in Northeastern Brazil and obtained $0.22 < \beta_1 < 0.38$ and $0.31 < \beta_2 < 0.58$. The values obtained in this study lie within the same intervals. Seasonal changes detected in this study were very small and were not taken into account when applying the model to the three stations, the same procedure adopted by Iziomon and Mayer [53] for the southeastern Germany and Almorox and Hontoria [3] for Toledo, Spain. Thus, it seems reasonable to fit the coefficients using annual averages rather than season dependent values [54]. Coefficients β_1 and β_2 depend on the latitude and longitude and this dependence is crucial in their fitting [55,56].

The coefficient of variation (cv) for the β_1 coefficient of M1 was 16.23% and 12.35% for β_2 at the three stations; these values differ from those of Liu et al. [57] for Chinese sites showing the dependence of the coefficients on local data and climate conditions. Values of $(\beta_1 + \beta_2)$ [0.725 (Água Branca), 0.714 (Pão de Açúcar) and 0.730 (Palmeira dos Índios)] showed the same trend with cv as small as 1.13%. The small differences among these values (less than 2.5%) can be explained recalling that the stations are within the tropical belt and the potential fraction of solar irradiation that impinges at the top of the atmosphere, that is, $(\beta_1 + \beta_2)$ for clear sky at the three stations is between 0.680 and 0.750 [58]. Tiba [6] obtained $0.58 < (\beta_1 + \beta_2) < 0.77$ for M1 when using with Brazil Northeastern data (small variability of cv = 6.8%). This result showed a similarity regarding its physical interpretation when atmospheric constituents (e.g. clouds, water vapor, aerosols) do affect the model (in particular β_1) coefficients. This sum for regions in the humid tropics is, generally, $0.670 < (\beta_1 + \beta_2) < 0.700$.

A significant negative correlation ($R = -0.996$; $p < 0.05$) between β_1 and altitude was observed for all sites. This coefficient was larger for the sites with a drier climate (Pão de Açúcar) than

Table 2
Empirical coefficients of the eleven models, using daily data, for the three stations in Alagoas.

Local	Model	Coefficients			
		β_1	β_2	β_3	β_4
Água Branca	M1	0.244*	0.481*	–	–
	M2	0.289*	0.293*	0.164*	–
	M3	0.265*	0.481*	–0.221*	0.234*
	M4	0.663*	0.209*	–	–
	M5	0.167*	0.567*	–0.042*	–
	M6	0.037*	0.266*	–	–
	M7	0.095*	0.137*	0.190*	–
	M8	0.304*	0.439*	1.345*	–
	M9	–1.218*	165.2*	–	–
	M10	0.550*	0.021*	–0.163*	–7.794*
	M11	12.4*	29.5*	–1.996*	–
Pão de Açúcar	M1	0.339*	0.375*	–	–
	M2	0.310*	0.496*	–0.103*	–
	M3	0.281*	0.707*	–0.526*	0.252*
	M4	0.677*	0.179*	–	–
	M5	0.414*	0.293*	0.041*	–
	M6	0.186*	0.203*	–	–
	M7	0.427*	0.579*	–0.112*	–
	M8	0.268*	0.436*	0.724*	–
	M9	–0.696*	119.6*	–	–
	M10	0.595*	0.008*	0.044*	11.4*
	M11	–36.6*	42.1*	–0.495*	–
Palmeira dos Índios	M1	0.297*	0.433*	–	–
	M2	0.290*	0.465*	–0.021*	–
	M3	0.278*	0.592*	–0.321*	0.188*
	M4	0.661*	0.146*	–	–
	M5	0.321*	0.406*	0.011*	–
	M6	0.105*	0.240*	–	–
	M7	0.322*	0.486*	–0.030*	–
	M8	0.282*	0.444*	0.922*	–
	M9	–0.971*	144.2*	–	–
	M10	0.553*	–0.065*	0.504*	0.182*
	M11	–6.7*	24.6*	–1.283*	–

* Significant at the 95% level.

for locations (Água Branca) with humid climate, differing in 38%. Since β_1 expresses the fraction of H_0 that reaches the Earth's surface on an overcast day (that is, the maximum fraction of H_d that may hit the surface), it increases with cloudiness. The larger the concentration of water vapor in the atmosphere the larger is the attenuation of the solar radiation thus yielding a larger value of β_1 for regions with a dry climate. Coefficient β_2 is positively correlated with altitude ($R = 0.999$; $p < 0.05$) and, negatively with latitude ($R = -0.817$; $p < 0.05$), while the correlation between $(\beta_1 + \beta_2)$ and altitude was smaller and positive ($R = 0.685$; $p < 0.05$). Since $(\beta_1 + \beta_2)$ did not change much from one site to another and, β_1 was larger for humid climates, β_2 showed an opposite pattern being larger in dry regions. $(\beta_1 + \beta_2)$ expresses the maximum fraction of H_0 that may reach the surface, what happens in clear sky conditions. These conditions were found for the three sites during the summer (dry) season (the sites are all located in interior where water content is small and shows no conspicuous changes). The smallness of the differences among $(\beta_1 + \beta_2)$ for the three sites is also explained by the short distances (less than 160 km) from each other what implies the same atmospheric composition and incident angles of solar radiation. The largest fractions of H_0 , under clear sky conditions, were observed at Palmeira dos Índios and Água Branca. This effect is associated with the local topography; Palmeira dos Índios is near the Borborema Plateau (hilly region spanning from Alagoas to Rio Grande do Norte, with an extension of 259 km) and Água Branca is at relatively high altitude (593 m). Therefore, the altitude effect may be responsible for the larger fraction of H_0 that reaches the surface [38]. The smallest value of $(\beta_1 + \beta_2)$ was for Pão de Açúcar, near São Francisco River,

thus indicating a moisture supply into the atmosphere even during the dry months. These coefficient relations are, in general, dependent on the location, weather systems and atmospheric chemistry (pollution, water vapor, rejects of industries and urban centers) [59].

Coefficient β_1 used in models M2, M3 and M8 also expresses the fraction of H_0 in a totally cloudy sky that reaches the surface, because when $n/N = 0$ (overcast sky) β_1 is smaller. The same sky conditions for models M6 and M7 results the sums $(\beta_1 + \beta_2)$ and $(\beta_1 + \beta_3)$, respectively, while for models M4 and M5, the atmospheric transmittance (k_t) is given by the vertical asymptote of the models (for $n/N \rightarrow 0$). The coefficient of variation for k_t in overcast days estimated for these models showed large values: 20.4% (Pão de Açúcar) and 21.6% (Palmeira dos Índios). This result was due to the large estimates given by M4 ($0.454 < k_t < 0.515$). The patterns for k_t in overcast days in M2, M3, M5, M6 and M7 were similar to that of M1, being smaller in regions of humid climate. In particular, M8 presented a reverse pattern with β_1 smaller in regions of dry climate. The atmospheric transmittance as estimated by M4 for Palmeira dos Índios (0.369) under completely cloudy sky was larger than that for Pão de Açúcar (0.319). The sum of the coefficients for M2 and M3 expresses the fraction of H_0 that reaches the surface in a cloudless day ($n/N = 1$), while in models M5 and M8, this fraction is given by the sum $(\beta_1 + \beta_2)$. The maximum atmospheric transmittance in M4 is given by β_1 and, by the horizontal asymptote ($n/N \rightarrow 1$) in models M6 and M7. The transmittance variability (cv for k_t) as given by the models, were for clear sky conditions: 2.6% (Pão de Açúcar) and 4.3% (Água Branca), that is, small dispersion of the estimated values. During the fitting of models M2, M3, M5, M6, M7 and M8, the maximum k_t increases from humid regions (Água Branca) to dry regions (Pão de Açúcar). The pattern was opposite in M4.

Coefficient β_1 of M2 was similar among the sites, with an averaged difference of 4.76%, while β_3 showed differences of 162% ($\beta_3 = -0.103$ at Pão de Açúcar and $\beta_3 = 0.164$ at Água Branca). This model reduces to model M1 when the coefficient β_3 of M2 tends to zero, as observed at Palmeira dos Índios ($\beta_3 = -0.021$). With respect to M1 for this same site, the differences among the estimates given by M2 for the same n/N were less than 2.5%. In general, the changes in β_1 and $(\beta_1 + \beta_2 + \beta_3)$ may be explained as consequences of local and seasonal conditions, type of clouds, concentration of water vapor and particulate material, altitude and latitude [3]. Coefficients β_3 of M3, M5 and M7 were negative. Coefficients β_1 and β_2 of models M2 to M8 ranged, respectively, in $0.037 < \beta_1 < 0.677$ (average 0.313 ± 0.164) and $0.137 < \beta_2 < 0.707$ (average 0.389 ± 0.155). Coefficient β_3 of models M2, M3, M5, M6 and M7 remained in the interval $-0.322 < \beta_3 < 1.345$ (average 0.512), while β_3 of M3 changed from 0.188 to 0.522 with an average of 0.225 ± 0.033 .

The spatial pattern shows that besides the altitude, other factors may exert an appreciable influence in the coefficient fitting stage. Água Branca has a more humid climate than that of the other stations due to topography-induced precipitation [49]. Water vapor is supplied into the region of Pão de Açúcar by the São Francisco River during most part of the year (the highly changeable water vapor concentration in the atmosphere is responsible by a larger absorption of infrared radiation, what lessens the global solar radiation). The fitted coefficients in this study were, in general, smaller than those of Li et al. [60] for regions in China. This discrepancy may be attributed to the local topography approximately ten times higher than that of Alagoas, thus implying a shorter optical path. Pollution and local effects apart, it is probable that these regions in China show less turbidity ($\beta_1 + \beta_2 \approx 0.868 \pm 0.041$) than in Alagoas. Persaud et al. [61] noticed that their model coefficients for Niger had a larger variability when particulate matter (aerosols and sand dust) was present in the

atmosphere. Ögelman et al. [20] found for their polynomial model (M2) when used in Turkey, the following averaged coefficients: $\beta_1 = 0.204$, $\beta_2 = 0.758$ and $\beta_3 = -0.250$. These values were different from those obtained in Alagoas. These coefficients were $\beta_1 = 0.340$, $\beta_2 = 0.400$ and $\beta_3 = 0.170$ as obtained by Newland [23] with the M5 model applied to coastal regions of southern China. Ampratwum and Dorvlo [22] found for the logarithmic model (M4) in Oman the coefficients β_1 (0.514–0.833) and β_2 (0.141–1.057), with R^2 (0.699–0.988); these were comparable to those obtained in this study. However, when they used the linear logarithmic model (M5) their coefficients [β_1 (–1.193–11.111), β_2 (–10.440–0.143) and β_3 (–1.254–9.665), with R^2 (0.735–0.996)] were different from those fitted for the Alagoas stations. Almorox and Hontoria [24] used the exponential model (M6) for different regions in Spain and obtained the coefficients $\beta_1 = -0.027$ and $\beta_2 = 0.309$; these values were also different from those obtained in Alagoas. They also fitted the coefficients of M4 for the same regions ($\beta_1 = 0.690$ – similar to ours, $\beta_2 = 0.614$ and $R^2 = 0.842$). Şen [26] used the model M8 for eight different sites in Turkey and found: $0.166 < \beta_1 < 0.429$, $0.223 < \beta_2 < 0.535$ and $1.940 < \beta_3 < 0.640$. The latter was quite close to the values obtained in this study. When the coefficients of models M9, M10 and M11 were compared with those of the original models of Bulut [40], Al-Salaymeh [41], Kaplanis and Kaplani [42], large differences were noticed [2], which may be attributed to the input variables. Although, the quality of the coefficient fitting was considered satisfactory, the results reinforced the need of fitting with local data.

Fitting with monthly averages

The coefficients fitted with monthly averages for the three sites, using the linear, polynomial, exponential, logarithmic and the proposed models are shown in Table 3. The monthly coefficients are also depended on the local climate conditions, like the daily coefficients. The coefficient β_1 of model M1 changed in the interval $0.163 < \beta_1 < 0.393$ (average = 0.265 ± 0.117 and $cv = 44.2\%$), β_2 in the interval $0.283 < \beta_2 < 0.582$ (average = 0.457 ± 0.155 and $cv = 34.0\%$) and $0.676 < (\beta_1 + \beta_2) < 0.746$ ($cv = 5.56\%$). The sum ($\beta_1 + \beta_2$) for monthly data showed differences ranging from –2.8% (at Água Branca) to 5.3% (at Pão de Açúcar), with respect to the values obtained with daily data. However, coefficient β_1 of the M1 was 15.8% smaller (at Pão de Açúcar) but 19.5% (at Palmeira dos Índios) and 33.2% (at Água Branca) larger than the corresponding ones obtained with daily data. Coefficients β_1 and β_2 of M2, M5, M7, M8 and M11 models for the regions of Água Branca and Palmeira dos Índios exhibited due to the geographical position and altitude of the sites, what is in agreement with results of Chen et al. [55] in China. El-Sebaili and Trabea [10] noticed that the coefficients β_1 and β_2 did not change much with respect to the latitude or altitude; however the sums ($\beta_1 + \beta_2$) were quite close to those obtained in Alagoas. Coefficient β_4 of M10 and β_3 of M11 were also similar to those observed at the three sites in Alagoas. The coefficient β_2 of models M9 and M11 showed the largest differences among the sites. The fitted coefficients for the stations in Alagoas differed from those used by Ångström [15] who suggested values of 0.20 and 0.50 for β_1 and β_2 , respectively. The FAO-56 Bulletin [62] recommends that for regions where there are no H_g data available, models with fixed values of $\beta_1 = 0.25$ and $\beta_2 = 0.50$ be used. The results obtained in this study are different from those just mentioned but agree with those of Chineke [18] what, again, reinforces the need for fitting with local data. It is worth mentioning that when monthly data are used to fit the coefficients of empirical models, large variations are likely to occur if the climatic series are not sufficiently long. Nevertheless, the fitted coefficients may still be used in models on a daily basis [38].

Table 3
Empirical coefficients for the eleven models at the 3 sites in Alagoas, using monthly data.

Local	Model	Coefficients			
		β_1	β_2	β_3	β_4
Água Branca	M1	0.163*	0.582*	–	–
	M2	0.079*	0.868*	–0.233*	–
	M3	–0.153*	2.046*	–2.167*	1.030*
	M4	0.695*	0.344*	–	–
	M5	0.454*	0.264*	0.189*	–
	M6	–0.059*	0.312*	–	–
	M7	0.340*	1.036*	–0.244*	–
	M8	–0.253*	0.970*	0.453*	–
	M9	–1.660*	205.4*	–	–
	M10	0.104*	0.703*	6.072*	6.287*
	M11	–4.2*	34.2*	–1.419*	–
Pão de Açúcar	M1	0.393*	0.283*	–	–
	M2	0.023*	1.459*	–0.902*	–
	M3	–0.169*	2.377*	–2.324*	0.717*
	M4	0.660*	0.185*	–	–
	M5	1.501*	–0.900*	0.753*	–
	M6	0.302*	0.143*	–	–
	M7	1.019*	2.068*	–0.925*	–
	M8	–17.389*	18.050*	0.010*	–
	M9	–0.488*	99.4*	–	–
	M10	–0.860*	1.473*	5.632*	7.0*
	M11	–9.1*	19.1*	–1.048*	–
Palmeira dos Índios	M1	0.239*	0.507*	–	–
	M2	0.137*	0.848*	–0.274*	–
	M3	–0.407*	3.578*	–4.690*	2.313*
	M4	0.705*	0.305*	–	–
	M5	0.600*	0.115*	0.236*	–
	M6	0.051*	0.268*	–	–
	M7	0.436*	1.026*	–0.276*	–
	M8	–1.001*	1.714*	0.198*	–
	M9	–1.345*	178.5*	–	–
	M10	–0.252*	1.025*	7.761*	6.7*
	M11	–7.3*	30.4*	–1.321*	–

* Significant at 95% level.

Under clear sky conditions ($n/N = 1$), the global atmospheric transmittance estimated by the models remained between 0.663 (M4) and 0.760 (M6) at Água Branca, 0.667 (M4) and 0.738 (M6) at Pão de Açúcar and 0.661 (M4) and 0.757 (M6) at Palmeira dos Índios. These values were similar to those presented in the literature and discussed in this study. The differences in the transmittances under these conditions were between –7.7% and 18.4% (on a daily basis). Models M3 and M8, under conditions of overcast sky yielded negative values, what is physically unacceptable. The global atmospheric transmittances obtained with M2 and M7, when $n/N = 0$, were all less than 0.160; less than 0.094 at Água Branca and Pão de Açúcar, values much lower than those found in the literature. Only M1, M4 and M6 models yielded comparable values under the same sky conditions. However, these coefficients were fitted using the least square error method and express the best statistical local fitting, that is, they have only statistical meaning.

The averaged differences between the daily and monthly coefficients for the three stations were large (average of 15%). Martinez-Losano et al. [63] noticed that the variability of the Ångström–Prescott coefficients is related to the geographical location and atmospheric conditions (e.g. water vapor and pollution). These factors may explain quite satisfactorily the changes in β_1 and β_2 for different locations but not the temporal changes at a given site [38]. The monthly coefficients were different from those found by Li et al. [60]. Bakirci [25] obtained $-0.034 < \beta_1 < 0.962$, $-0.737 < \beta_2 < 2.67$ and $-1.12 < \beta_3 < 0.47$ for some sites in Turkey, with determination coefficient $0.127 < R^2 < 0.995$. The fitted coefficients of M2 are different from those proposed by Ögelman et al.

[20] ($\beta_1 = 0.195$, $\beta_2 = 0.676$ and $\beta_3 = -0.142$). The coefficients of the cubic model (M3) differ from those suggested by Bahel et al. [21] for 48 sites throughout the world ($\beta_1 = 0.160$, $\beta_2 = 0.870$, $\beta_3 = -0.610$ and $\beta_4 = 0.340$) and also different from those obtained by Samuel [64] in Sri Lanka ($\beta_1 = -0.140$, $\beta_2 = 2.52$, $\beta_3 = -3.71$ and $\beta_4 = 2.24$). The monthly coefficients of M4 were similar to those proposed by Ampratwum and Dorvlo [22] ($\beta_1 = 0.637$ and $\beta_2 = 0.249$).

Statistical performance of the models on a daily basis

The statistical indices to measure the model performance in estimating H_g^d for the sites in Alagoas are shown in Table 4. All models showed estimates with $|\text{MBE}| < 0.94 \text{ MJ m}^{-2}$, $\text{RMSE} < 4.51 \text{ MJ m}^{-2}$ and $d > 0.70$. For the region of Água Branca $-0.55 < \text{MBE} < 0.38 \text{ MJ m}^{-2}$, $2.93 < \text{RMSE} < 4.51 \text{ MJ m}^{-2}$ and $0.66 < d < 0.93$; M11 yielded for this region, the smallest values of MBE (0.31 MJ m^{-2}) and RMSE (2.93 MJ m^{-2}). M10 had the largest RMSE (4.51 MJ m^{-2}) and smallest d (0.66) followed by M3 with $\text{RMSE} = 3.12 \text{ MJ m}^{-2}$ and $d = 0.89$. These models (M3 and M10) showed estimates statistically different from the H_g^d observations. M1 yielded $\text{MBE} = -0.55 \text{ MJ m}^{-2}$, $\text{RMSE} = 3.0 \text{ MJ m}^{-2}$ and $d = 0.92$. All but the M3 and M11 models underestimated the measurements (average of $-0.54 \pm 0.05 \text{ MJ m}^{-2}$) in Água Branca region. In general, the proposed models (M9, M10 and M11) showed a dispersion 2.74% larger than those of the remaining empirical models (M1–M8); this is due to the large (the largest of them all) $\text{RMSE} = 1.53 \text{ MJ m}^{-2}$ of model M10. The estimates obtained with models M1 and M11 do not differ statistically by more than 5%. However, models M9 and M11 have skill superior or equal to those of the others. These results are better than those of [65] who proposed new models to estimate the global solar irradiation in China with $1.71 < \text{RMSE} < 5.24 \text{ MJ m}^{-2}$ and [66] for some sites within the Yangtze Basin, also in China, with $1.81 < \text{RMSE} < 3.39 \text{ MJ m}^{-2}$.

The RMSE values for Água Branca were larger than those for Pão de Açúcar and Palmeira dos Índios. This reflects the fact that the dispersion increased with the cloudiness associated with the microclimate of Água Branca region. The increase in the errors due to increasing cloudiness stems from the strong relation between incident solar radiation and cloud coverage. The results for the Pão de Açúcar region showed smaller values of MBE and RMSE, when M3 is used; the estimates obtained with this model differ no more than 5% of the measurements. The statistical indices MBE and RMSE of models M1, M9 and M11 were all similar, with high agreement (averaged $d = 0.92 \pm 0.22$). RMSE at Pão de Açúcar was larger than that of Palmeira dos Índios, probably due to the more humid climate of the former station (recall Pão de Açúcar is at the margins of São Francisco River). All the models overestimated the measurements for the region of Palmeira dos Índios, in particular M3 and M10 which yielded the largest and smallest

MBE, respectively. The cubic, logarithmic and sinusoidal models (M3, M4 and M10, in this order) showed the largest RMSE. Despite its small MBE, M10 showed the largest dispersion ($\text{RMSE} = 3.55 \text{ MJ m}^{-2}$) and smallest agreement ($d = 0.78$). The analysis of the MBE showed that M1 overestimated the measurements by 0.22 MJ m^{-2} (1.1%), with a dispersion of 1.95 MJ m^{-2} (9.7%) and $d = 0.96$. These indices show that the estimates follow the variability of the measurements, with small dispersion and large index of agreement. The results also showed that the performance of the models is satisfactory mainly for the sinusoidal models M9 and M11. Although, the original Ångström–Prescott model (M1) is more often recommended due to its simplicity and practicability, models M9 and M11 have their own advantages for they produce errors smaller than those of M1. Models M2, M9 and M19 are all statistically similar.

Fig. 4 shows the dispersion for model M1 and the models that yielded the best and worst estimates according to RMSE values. Models M1 and M11 showed small dispersion for the region of Água Branca, with most of the points clustered along the ideal straight line of model comparisons (1:1), M10 showed the highest dispersion with no satisfactory linear fitting (Fig. 4A). The dispersion using model M10 for Pão de Açúcar (Fig. 4B) and Palmeira dos Índios (Fig. 4C) was large, while for these two sites M1, M3 and M9 models yielded the best estimates.

These results showed that the adjustments made for the Alagoas sites were statistically better than those [67]. The authors mention as examples of high correlations, the significant correlations at Chaoyang ($R = 0.969$; $p < 0.001$), Dalian ($R = 0.971$; $p < 0.001$) and Shengyang ($R = 0.967$; $p < 0.001$). This statement agrees with the results obtained in Alagoas: Água Branca ($R = 0.977$; $p < 0.0001$), Pão de Açúcar ($R = 0.982$; $p < 0.0001$) and Palmeira dos Índios ($R = 0.975$; $p < 0.0001$). Zhou et al. [68] obtained better estimates for some sites in China using the logarithmic model (M4) while in the present study the better estimates in Água Branca and Pão de Açúcar were achieved with the cubic model (M3), and the sinusoidal model (M11) for Palmeira dos Índios. In general, the local results were analogous to those obtained by [68]. Many studies have utilized the Ångström–Prescott model (M1) and its versions to correlate the global solar radiation with the sunshine at different time scales: daily [60,69–71] and monthly [60]. Yao et al. [72] estimated hourly H_g from daily data. It is worthwhile mentioning the satisfactory results attained with M9 and M11 models for the stations in Alagoas.

Statistical performance of the models on a monthly basis

Among the modified versions of the Ångström–Prescott model (M1), the quadratic (M2) and cubic (M3) models yielded the largest RMSE and MBE and the smallest d when monthly data are used

Table 4
Statistical indices for the models with daily data: MBE (Mean Bias Error) and RMSE (Root Mean Square Error) in MJ m^{-2} and d (Willmott index of agreement).

Model #	Model	Água Branca			Pão de Açúcar			Palmeira dos Índios		
		MBE	RMSE	d	MBE	RMSE	d	MBE	RMSE	d
M1	Linear	-0.55	2.98	0.92	-0.91	2.11	0.94	0.22	1.95	0.96
M2	Quadratic	-0.45	2.96	0.93	-0.87	2.08	0.94	0.20	1.95	0.96
M3	Cubic	0.38	2.96	0.93	0.16	1.93	0.95	0.94	2.23	0.95
M4	Logarithmic	-0.51	3.12	0.89	-0.83	2.14	0.94	0.27	2.47	0.93
M5	Linear logarithmic	-0.55	2.99	0.92	-0.88	2.09	0.94	0.23	1.96	0.96
M6	Exponential	-0.54	2.97	0.92	-0.89	2.15	0.94	0.17	1.95	0.96
M7	Linear exponential	-0.52	2.96	0.92	-0.87	2.08	0.94	0.22	1.96	0.96
M8	Power	-0.52	2.97	0.92	-0.90	2.10	0.94	0.23	1.96	0.96
M9	Sinusoidal	-0.65	2.99	0.92	-0.80	2.10	0.94	0.14	1.90	0.96
M10	Sinusoidal	-0.55	4.51	0.66	-0.77	3.55	0.70	0.05	3.55	0.78
M11	Sinusoidal	0.31	2.93	0.93	-0.78	2.09	0.94	0.51	1.97	0.96

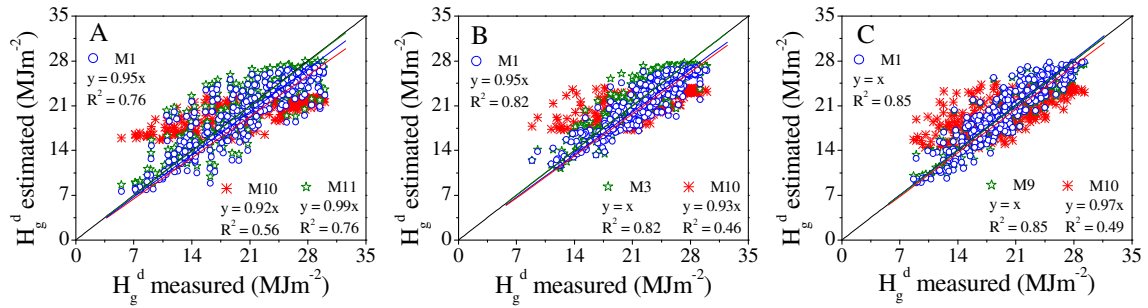


Fig. 4. Dispersions of the best and worst estimates of daily global solar irradiation (H_g^d) obtained for (A) Água Branca, (B) Pão de Açúcar e (C) Palmeira dos Índios.

Table 5

Monthly statistical indices: MBE (Mean Bias Error) and RMSE (Root Mean Square Error) in MJ m^{-2} ; d (Willmott index).

Model #	Model	Água Branca			Pão de Açúcar			Palmeira dos Índios		
		MBE	RMSE	d	MBE	RMSE	d	MBE	RMSE	d
M1	Linear	-0.95	1.48	0.97	-0.97	1.25	0.96	-1.17	1.65	0.95
M2	Quadratic	-0.98	1.45	0.97	-0.87	1.13	0.97	-11.18	11.71	0.32
M3	Cubic	3.82	4.11	0.84	2.64	2.78	0.85	10.13	10.33	0.43
M4	Logarithmic	-1.05	1.45	0.97	-0.92	1.19	0.97	-1.16	1.54	0.95
M5	Linear logarithmic	-1.01	1.46	0.97	-0.82	1.08	0.97	-1.14	1.55	0.95
M6	Exponential	-0.86	1.52	0.97	-0.93	1.23	0.96	-1.20	1.73	0.94
M7	Linear exponential	-0.94	1.42	0.97	-0.82	1.10	0.97	-1.09	1.54	0.96
M8	Power	-0.98	1.44	0.97	-0.81	1.11	0.97	-1.15	1.56	0.95
M9	Sinusoidal	-0.92	1.47	0.97	-0.93	1.22	0.96	-1.16	1.64	0.95
M10	Sinusoidal	-0.99	1.45	0.97	-0.85	1.12	0.97	-1.16	1.58	0.95
M11	Sinusoidal	-0.91	1.46	0.97	-0.92	1.21	0.97	-0.57	1.32	0.97

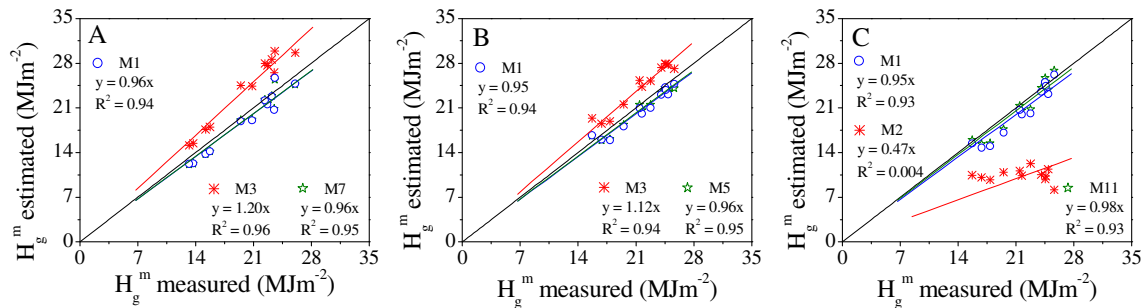


Fig. 5. Dispersions of the best and worst estimates of monthly global solar irradiation (H_g^m) obtained for (A) Água Branca, (B) Pão de Açúcar e (C) Palmeira dos Índios.

(Table 5). These results differed from those of Zhou et al. [68] who obtained smaller errors for M2 and M3 using local Chinese data; Yorukoglu and Celtik [73] who obtained for these models RMSE quite close to that of the linear model (M1). This may be due to the fact that the models were not appropriately fitted to the local conditions. In general, the more coefficients an empirical model has the higher the chances to yield a better performance [67]. However, changes introduced in the quadratic (M2), cubic (M3), logarithmic (M4), linear logarithmic (M5), exponential (M6), linear exponential (M7) and power (M8) models did not improve their performances with the linear model M1 used as standard. The modifications in the sinusoidal models (M9, M10 and M11) made their performances comparable or even better than that of M1. The statistical index MBE showed that all models underestimated the observations at Água Branca, with the exception of M3 which overestimated the measurements in 3.82 MJ m^{-2} ; with $1.42 < \text{RMSE} < 4.11 \text{ MJ m}^{-2}$ and $0.84 < d < 0.97$.

A MBE analysis showed that all (but one) models underestimated the measurements at Pão de Açúcar. Model M3 overestimated the observations in 2.64 MJ m^{-2} with $1.08 < \text{RMSE} < 2.78 \text{ MJ m}^{-2}$ and

$0.85 < d < 0.97$. The linear model (M1) yielded small errors ($\text{MBE} = -0.97 \text{ MJ m}^{-2}$ and $\text{RMSE} = 1.25 \text{ MJ m}^{-2}$), with a large agreement index ($d = 0.97$). The best performance for this region was achieved with M10 ($\text{MBE} = -0.85 \text{ MJ m}^{-2}$, $\text{RMSE} = 1.12 \text{ MJ m}^{-2}$ and $d = 0.97$). The same was observed for the region of Palmeira dos Índios, with M3 being the only model that overestimated the measurements ($\text{MBE} = 10.13 \text{ MJ m}^{-2}$); for the others, $-11.18 < \text{MBE} < -0.57 \text{ MJ m}^{-2}$. The largest dispersions were found with M2 and M3 models, with $\text{RMSE} = 11.71$ and 10.33 MJ m^{-2} , respectively. For the others the RMSE remained in the interval $1.32 < \text{RMSE} < 1.73 \text{ MJ m}^{-2}$ with an average of $1.57 \pm 0.11 \text{ MJ m}^{-2}$. Index d was large for M11 (0.97) but small for M2 (0.32), with an overall average of $d = 0.85 \pm 0.24$. The estimates obtained with M11 were statistically similar to the observations. The local results are similar to those found by Ertekin and Evrendilek [74] in Turkey with the exponential model ($\text{RMSE} = 1.62 \text{ MJ m}^{-2}$), logarithmic model ($\text{RMSE} = 1.59 \text{ MJ m}^{-2}$) and the linear logarithmic ($\text{RMSE} = 1.59 \text{ MJ m}^{-2}$) but differed from those of the quadratic model ($\text{RMSE} = 1.58 \text{ MJ m}^{-2}$) and cubic model ($\text{RMSE} = 1.59 \text{ MJ m}^{-2}$). The monthly results are similar to those of Li et al.

[66] for sites in the Tangtze River Basin in China with $0.70 < \text{RMSE} < 1.98 \text{ MJ m}^{-2}$. The M1 dispersion together with those of the models that yielded the best and worst estimates are shown in Fig. 5A–C. M3 and M2 showed the largest dispersions for the regions of Água Branca and Palmeira dos Índios, respectively.

The patterns obtained with monthly indices differed from those with daily indices. Long term series of monthly averaged data may be useful to seek better correlations between H_g and sunshine, since daily data are vulnerable to local weather and air pollution (responsible for fewer hours of sunshine and less solar radiation reaching the surface [68]). It was noticed that all empirical models had a satisfactory performance for all regions, except M2 (in Palmeira dos Índios) and M3 (in the three stations). It is important to emphasize that: (a) atmospheric pollution can affect the H_g estimates and (b) the proposed models (M9, M10 and M11) also yielded good estimates.

Conclusions

Reliable data of H_g are of great importance for growth models, agricultural productivity projects and feasibility studies for the installation of solarimetric plants. The time and space variability of H_g is instrumental for decision makers and establishment of policies regarding agricultural and energetic practices. Eleven empirical models using sunshine duration as input data to estimate H_g^d and H_g^m were assessed for three sites in Alagoas State, NEB. The study also took into account the presence of clouds and their effects in the atmosphere energy budget.

The seasonal variations found in k_t , n/N and Φ depend on the local condition of cloudiness, (being larger during the winter), particulate material due to slash burnings of biomass and adjacent vegetation (mainly during summer) besides the import of water vapor due to the proximity to the coastline. The cloudiness ratio (Φ) is larger (smaller) in the rainy (dry) periods, in accordance with the pluviometric indices. A larger number of overcast days and, consequently smaller transmittance characterizes the rainy season; the opposite is true for the dry period.

Different coefficients β_1 and β_2 of the original Ångström–Prescott (M1) model are used depending on whether a daily or monthly basis is desired. However, they indicate the same potential fraction of global solar irradiation with respect to that at the top of atmosphere ($\beta_1 + \beta_2 = 0.74$) in clear days, as a function of the climate characteristics and atmospheric composition of the regions chosen in this study. β_1 is larger for humid than dry climate and also reveals a dependence on the altitude while β_2 is a function of both latitude and altitude. Besides its good performance, this has coefficients which can be physically interpreted.

The original M1 and the cosenoidal wave model (M11) after fitted with local data yielded better estimates of the solar global irradiation with higher accuracy and precision than the remaining models (M2–M10). Sunshine duration data (for estimating global solar irradiation estimates for sites such as Água Branca, Pão de Açúcar, Palmeira dos Índios, and probably other regions with similar micro climates) may be a solution to the data shortage problem when there are no H_g measurements available. Therefore, the M1 and M11 models are highly recommended to be used in a data bank of global solar irradiation for sites where H_g measurements are not available or scarce. These models will allow researchers, engineers and decision making people to utilize the estimates with a high level of confidence.

Acknowledgements

Our thanks to the Instituto Nacional de Meteorologia (INMET), Coordenação de Aperfeiçoamento de Pessoal de Nível Superior

(CAPES), Eletrobrás (Centrais Elétricas Brasileiras S. A.) and CNPq (Conselho Nacional de Desenvolvimento Científico e Tecnológico).

References

- [1] Santos CM, Souza JL, Teramoto ET, Tiba C, Melo RO. Modelagem da irradiação solar global média horária mensal (h_g^m) para quatro localidades de Alagoas/Brasil. *Nativa* 2014;02(02):79–88 [Sinop, abr./jun., in portuguese].
- [2] Li H, Ma W, Lian Y, Wang X. Estimating daily global solar radiation by day of year in China. *Appl Energy* 2010;87:3011–7.
- [3] Almorox J, Benito M, Hontoria C. Estimation of monthly Ångström–Prescott equation coefficients from measured daily data in Toledo, Spain. *Renewable Energy* 2005;30:931–6.
- [4] Donnelly JR, Moore AD, Freer M. Grazplant: decision support systems for Australian grazing enterprises. I. Overview of the GRAZPLANT project, and a description of the MetAccess and LambAlive DSS. *Agric Syst* 1997;54:57–76.
- [5] Thornton PE, Running SW. An improved algorithm for estimating incident daily solar radiation from measurements of temperature, humidity, and precipitation. *Agric For Meteorol* 1999;93:211–28.
- [6] Tiba C. Solar radiation in the Brazilian Northeast. *Renewable Energy* 2001;22(4):565–78.
- [7] Codato G, Oliveira AP, Soares J, Escobedo JF, Gomes EN, Dal Pai A. Global and diffuse solar irradiances in urban and rural areas in southeast Brazil. *Theor Appl Climatol* 2008;93:57–73.
- [8] Martins FR, Pereira EB, Abreu SL. Satellite-derived solar resource maps for Brazil under SWERA project. *Sol Energy* 2007;81:517–28.
- [9] Santos CM, Souza JL, Ferreira Junior RA, Tiba C, Melo RO, Lyra GB, Teodoro I, Bastos Lyra G, Lemes MAM. On modeling global solar irradiation using air temperature for Alagoas State, Northeastern Brazil. *Energy* 2014;71:388–98.
- [10] El-Sebaei AA, Trabea AA. Estimation of global solar radiation on horizontal surfaces over Egypt. *Egypt J Solids* 2005;28(1):163–75.
- [11] Bristow KL, Campbell GS. On the relationship between incoming solar radiation and daily maximum and minimum temperature. *Agric For Meteorol* 1984;31:159–66.
- [12] Hargreaves GH, Samani ZA. Estimating potential evapotranspiration. *J Irrig Drain Eng* 1982;108:225–30.
- [13] Trabea AA, Shaltou M. Correlation of global solar radiation with meteorological parameters over Egypt. *Renewable Energy* 2000;21(2):297–308.
- [14] Winslow JC, Hunt Jr ER, Piper SC. A globally applicable model of daily solar irradiance estimated from air temperature and precipitation data. *Ecol Model* 2001;143(3):227–43.
- [15] Ångström A. Solar and terrestrial radiation. *Q J R Meteorol Soc* 1924;50:121.
- [16] Prescott JA. Evaporation from a water surface in relation to solar radiation. *Trans R Soc Sci Aust* 1940;64:114–25.
- [17] Bakirci K. Models of solar radiation with hours of bright sunshine: a review. *Renewable Sustainable Energy Rev* 2009;13(9):2580–8.
- [18] Chineke TC. Equations for estimating global solar radiation in data sparse regions. *Renewable Energy* 2008;33:827–31.
- [19] Al-Mohamad A. Global, direct and diffuse solar-radiation in Syria. *Appl Energy* 2004;79:191–200.
- [20] Ögelman H, Ecevit A, Tasemiroglu E. A new method for estimating solar radiation from bright sunshine data. *Sol Energy* 1984;33:619–25.
- [21] Bahel V, Bakhsh H, Srinivasan R. A correlation for estimation of global solar radiation. *Energy* 1987;12:131–5.
- [22] Ampratwum DB, Dorvlo ASS. Estimation of solar radiation from the number of sunshine hours. *Appl Energy* 1999;63:161–7.
- [23] Newland FJ. A study of solar radiation models for the coastal region of South China. *Sol Energy* 1989;43:227–35.
- [24] Almorox J, Hontoria C. Global solar radiation estimation using sunshine duration in Spain. *Energy Convers Manage* 2004;45:1529–35.
- [25] Bakirci K. Correlations for estimation of daily global solar radiation with hours of bright sun shine in Turkey. *Energy* 2009;34:485–501.
- [26] Şen Z. Simple nonlinear solar irradiation estimation model. *Renewable Energy* 2007;32:342–50.
- [27] Güçlü YS, Yeleğen MÖ, Dabanlı I, Şişman E. Solar irradiation estimations and comparisons by ANFIS, Ångström–Prescott and dependency models. *Sol Energy* 2014;109:118–24.
- [28] Rehman S, Halawani TO. Global solar radiation estimation. *Renewable Energy* 1997;12(4):369–85.
- [29] Al-Mostafa ZA, Maghrabi AH, Al-Shehri SM. Sunshine-based global radiation models: a review and case study. *Energy Convers Manage* 2014;84:209–16.
- [30] Mota FS, Beirsdorf MIC, Acosta MJ. Estimates of solar radiation in Brazil. *Agric Meteorol* 1977;18:241–54.
- [31] Tiba C, Aguiar R, Fraidenaich N. Analysis of a new relationship between monthly global irradiation and sunshine hours from a database of Brazil. *Renewable Energy* 2005;30:957–66.
- [32] Tiba C, Fraidenaich N. Analysis of monthly time series of solar radiation and sunshine hours in tropical climates. *Renewable Energy* 2004;29:1147–60.
- [33] Andrade-Júnior AS, Noletto DH, da Silva ME, Braga DL, Bastos EA. Coeficientes da equação de Ångström–Prescott para Parnaíba, Piauí. *Comunicata Scientiae* 2012;3(1):50–4 [in portuguese].
- [34] Jerszurki D, Souza JLMD. Parametrização das equações de Hargreaves & Samani e Ångström–Prescott para estimativa da radiação solar na região de Telêmaco Borba, estado do Paraná. *Ciência Rural* 2013;43(3):383–9 [in portuguese].

- [35] Daniele K, Dornelas S, da Silva CL, da Silva CAO. Coeficientes médios da equação de Ångström–Prescott, radiação solar e evapotranspiração de referência em Brasília. *Pesq Agropec Bras* 2006;41(8):1213–9 [in portuguese].
- [36] Carvalho DFD, Silva DG, Souza APD, Gomes DP, Rocha HSD. Coeficientes da equação de Ångström–Prescott e sua influência na evapotranspiração de referência em Seropédica, RJ. *Rev Bras Eng Agríc Ambient* 2011;15(8):838–44 [in portuguese].
- [37] Ångström A. On the computation of global radiation from records of sunshine. *ArkivFörGeofysik* 1956;2(22):471.
- [38] Liu X, Mei X, Li Y, Zhang Y, Wang Q, Jensen JR, Porter JR. Calibration of the Ångström–Prescott coefficients (a, b) under different time scales and their impacts in estimating global solar radiation in the yellow River basin. *Agric For Meteorol* 2009;149:697–710.
- [39] Duffie J, Beckman WA. *Solar engineering of thermal processes*. 3rd ed. New York; 2006, p. 928.
- [40] Bulut H. Generation of typical solar radiation data for Istanbul, Turkey. *Int J Energy Res* 2003;27:847–55.
- [41] Al-Salaymeh A. Model for the prediction of global daily solar radiation on horizontal surfaces for Amman city. *Emirates J Eng Res* 2006;11:49–56.
- [42] Kaplanis S, Kaplani E. A model to predict expected mean and stochastic hourly global solar radiation I(h;nj) values. *Renewable Energy* 2007;32:1414–25.
- [43] Souza JL, Nicácio RM, Moura MAL. Global solar radiation measurements in Maceió, Brazil. *Renewable Energy* 2005;30:1203–20.
- [44] Teramoto ET, Escobedo JF. Análise da frequência anual das condições de céu em Botucatu, São Paulo. *Rev Bras Eng Agríc Ambient* 2012;16(9):985–92 [in Portuguese].
- [45] Iqbal M. Prediction of hourly diffuse solar radiation from measured hourly global radiation on a horizontal surface. *Sol Energy* 1980;24:491–503.
- [46] Willmott CJ. On the validation of models. *Phys Geogr* 1981;2(2):184–94 [Delaware].
- [47] Escobedo JF, Gomes EN, Oliveira AP, Soares J. Ratios of UV, PAR and NIR components to global solar radiation measured at Botucatu site in Brazil. *Renewable Energy* 2011;36:169–78.
- [48] World Meteorological Organization (WMO). *Guide to meteorological instruments and methods of observation*. 7th ed. Geneva: n. 8; 2008, p. 681.
- [49] Lyra GB, Oliveira-Júnior JF, Zeri M. Cluster analysis applied to the spatial and temporal variability of monthly rainfall in Alagoas state, Northeast of Brazil. *Int J Climatol* 2014;34:3546–58.
- [50] Jiang Y. Correlation for diffuse radiation from global solar radiation and sunshine data at Beijing, China. *J Energy Eng* 2009;135:107–11.
- [51] Tymvios FS, Jacovides CP, Michaelides SC, Scouteli C. Comparative study of Ångström's and artificial neural networks' methodologies in estimating global solar radiation. *Sol Energy* 2005;78:752–62.
- [52] Podestá GP, Núñez L, Villanueva CA, Skansi MA. Estimating daily solar radiation in the Argentine Pampas. *Agric For Meteorol* 2004;123:41–53.
- [53] Iziomon MG, Mayer H. Assessment of some global solar radiation parameterizations. *J Atmos Solar Terr Phys* 2002;64:1631–43.
- [54] Liu XY, Mei XR, Li YZ, Porter JR, Wang QG, Zhang YQ. Choice of the Ångström–Prescott coefficients: are time-dependent ones better than fixed ones in modeling global solar irradiance? *Energy Convers Manage* 2010;51:2565–74.
- [55] Chen R, Lu S, Kang E, Yang J, Ji X. Estimating daily global radiation using two types of revised models in China. *Energy Convers Manage* 2006;47:865–78.
- [56] Jin Z, Wu Y, Yan G. General formula for estimation of monthly average daily global solar radiation in China. *Energy Convers Manage* 2005;46:257–68.
- [57] Liu X, Wu Y, Zhong X, Zhang W, Porter JR, Liu W. Assessing models for parameters of the Ångström–Prescott formula in China. *Appl Energy* 2012;96:327–38.
- [58] Akpabio LE, Etuk SE. Relationship between global solar radiation and sunshine duration for Onne, Nigeria. *Turkey J Phys* 2003;27:161–7.
- [59] Adaramola MS. Estimating global solar radiation using common meteorological data in Akure, Nigeria. *Renewable Energy* 2012;47:38–44.
- [60] Li H, Ma W, Lian Y, Wang X, Zhao L. Global solar radiation estimation with sunshine duration in Tibet, China. *Renewable Energy* 2011;36:3141–5.
- [61] Persaud N, Lesolle D, Ouattara M. Coefficients of the Ångström–Prescott equation for estimating global irradiance from hours of bright sunshine in Botswana and Niger. *Agric For Meteorol* 1997;88:27–35.
- [62] Allen R, Pereira LS, Raes D, Smith M. *Crop evapotranspiration–Guidelines for Computing Crop Water Requirements – FAO Irrigation and Drainage Paper 56, Food and Agriculture Organization of the United Nations, Rome; 1998, p. 300.*
- [63] Martínez-Lozano JA, Tena F, Onrubia JE, De La Rubia J. The historical evolution of the Ångström formula and its modifications: review and bibliography. *Agric For Meteorol* 1984;33:109–28.
- [64] Samuel TDMA. Estimation of global radiation for Sri Lanka. *Sol Energy* 1991;47:333–7.
- [65] Zhao N, Zeng X, Han S. Solar radiation estimation using sunshine hour and air pollution index in China. *Energy Convers Manage* 2013;76:846–51.
- [66] Li M-F, Fan L, Liu H-B, Wu W, Chen J-J. Impact of time interval on the Ångström–Prescott coefficients and their interchangeability in estimating radiation. *Renewable Energy* 2012;44:431–8.
- [67] Chen J-L, Li G-S, Wu S-J. Assessing the potential of support vector machine for estimating daily solar radiation using sunshine duration. *Energy Convers Manage* 2013;75:311–8.
- [68] Zhou J, Wu YZ, Yan G. General formula for estimation of monthly average daily global solar radiation in China. *Energy Convers Manage* 2005;46:257–68.
- [69] Chen R, Kang E, Yang J, Lu S, Zhao W. Validation of five global radiation models with measured daily data in China. *Energy Convers Manage* 2004;45:1759–69.
- [70] Li M, Tang X, Wu W, Liu H. General models for estimating daily global solar radiation for different solar radiation zones in mainland China. *Energy Convers Manage* 2013;70:139–48.
- [71] Güçlü YS, Dabanlı I, Şişman E, Şen Z. HARMONICLINear (HarLin) model for solar irradiation estimation. *Renewable Energy* 2015;81:209–18.
- [72] Yao W, Li Z, Xiu T, Lu Y, Li X. New decomposition models to estimate hourly global solar radiation from the daily value. *Sol Energy* 2015;120:87–99.
- [73] Yorukoglu M, Celik AN. A critical review on the estimation of daily global solar radiation from sunshine duration. *Energy Convers Manage* 2006;47:2441–50.
- [74] Ertekin C, Evrendilek F. Spatio-temporal modeling of global solar radiation dynamics as a function of sunshine duration for Turkey. *Agric For Meteorol* 2007;145:36–47.